RESULTS OF THE EXPERIMENT "PAMIR" AND THE STRONG INTERACTION MODEL AT ENERGY HIGHER THAN 10^{15} eV

Rauf A.Mukhamedshin

Institute for Nuclear Research
Russian Academy of Sciences

Summary

Results of the Collaboration "Pamir" and nuclear-electromagnetic cascade simulations based on a quark-gluon string model are discussed. Conclusions on a rather good agreement between the total set of data and simulation predictions are given. Model modifications are proposed by the author to improve the description of experimental data.

1. INTRODUCTION

In spite of the complexity of methodical problems of emulsion chamber (EC) investigations of the Collaboration "Pamir" [1], our understanding of multiple generation processes in hadron-nucleus interactions at $E>10^{15}$ eV is much better than it was 20 years ago. At present there is no need to discuss both a high multiplicity hypothesis or a CKP-like model and a pure scaling interaction picture although for a long time these models as well as a number of others [2] played an important role in cosmic ray physics. As a result we can conclude [3,4] that predictions based on a most improved theoretical quark-gluon string model (QGSM) [5] give the best description of the total experimental data, both characteristics of gamma-ray - hadron families (groups of correlated high-energy particles) and single component. Thus it is rational to discuss strong interaction characteristics on the basis of QGSM predictions. However, some experimental results cannot be easily explained within its frames. These problems are discussed below.

2. Some characteristics of QGSM and simulation algorithms

At present the Collaboration "Pamir" uses two computer QGSM-based algorithms to simulate nuclear-electromagnetic cascades (NEC), namely so-called models MQ [6] (and its version MQ1) and MC0 [7]. The models have many common properties, namely the inelastic cross-section $\sigma_{inel}^{h\text{-}air}$ and inelasticity coefficient $K_{inel}^{h\text{-}air}$ in hadron-air nucleus interactions increasing with energy; a moderate steepening of secondary particle generation spectra in the fragmentation region with energy increase. Diffraction

processes are taken into account; the creation of not only pions but also of other types of particles occurs. There are some differences in the models. Particularly, MQ simulates various diffraction channels and has an effective mechanism of parameter modification. The model MCO treats a larger set of particle types and takes into account and semi-hard jet generation as well as a few nontrivial processes [34]. These models reproduce inclusive spectra predicted by QGSM [5] as well as realize experimental fluctuations. For example, the multiple generation in MCO can carry out through the diffractive dissociation with a multiplicity $<n_{diff}(s)>$ and a relatively hard particle spectrum, or soft processes ($<n> \approx 2\cdot<n_{diff}>$, or jet generation accompanied by soft processes ($<n> \approx 4\cdot<n_{diff}>$. The most important difference between MQ and MCO is the pion inelastic charge-exchange (πICE) process $\pi^{ch} \to \pi^0$ with probability W_c=0.72 (0.5) taken into account only by MQ (MQ1) as well as the smaller value of $K_{inel}^{h\text{-}air}$ in MCO ($\cong$0.7 instead of $\cong$0.8 at E$\geq$10 PeV) [35].

Main differences of the models MSF [2,35] and MCP [45] will be mentioned below from the above models are $K_{inel}^{h\text{-}air} \approx 0.5$ in MSF and $K_{inel}^{h\text{-}air}$ decreasing with energy to $\cong$0.4 in MCP. Both models simulate pions only as secondaries.

3.ON COMPARISON OF EXPERIMENTAL AND SIMULATION RESULTS

A comparison of simulation predictions with emulsion experiment results is reasonable with simulations of detection processes only. It requires good computer programs and a lot of time. Thus, at present, predictions of MQ are compared with results obtained in so-called carbon emulsion chambers (C-EC) [8]. Predictions of MCO are analyzed only together with lead chamber (Pb-EC) data [3]. Two sets of partial inelasticity coefficients (K_γ^1 and K_γ^2), i.e. parts of energy transferred by hadrons into the electromagnetic (EM) component in h-Pb interactions, are used. In first case only π^0-generation is taken into account whereas in second case η-meson creation additionally is. A comparison of the results of MQ and MCO models is not easy.

Note the importance of a correspondence between models used for NEC simulations in the air and in chambers. Particularly, $K_{inel}^{h\text{-}air}$ has to be close to $K_{inel}^{h\text{-}carbon}$. In the opposite case results on hadron spectra cannot be correct [9,46].

4. PRIMARY COSMIC RAY SPECTRUM

Both the slope and chemical composition of the primary cosmic ray (PCR) spectrum are very important for EC experiments. The investigations [10,11] carried out within the framework of the Collaboration "Pamir" concluded that at $E \gtrsim 10^{15}$ eV the chemical composition is normal [10] and the fraction of iron nuclei does not exceed 27% [11]. JACEE [12] measurements give evidences in favor of a small increase of the proton integral spectrum index up to $\beta \approx 1.75 \div 1.85$. On the other hand, the analysis [46] shows that joint description of EAS and γ-h family characteristics is possible only by means of normal- composition PCR. Results [49,50] give evidences in favor of this conclusion. So we assume the normal chemical composition of PCR. Both MQ and MCO use primary spectra close to the so-called Nikolsky spectrum [15]. In simulations [3] two following proton spectrum fits are used:

$$I(>E/TeV)=2.69\cdot10^{-4}\cdot(E/0.1)^{-1.63}\cdot(1+6\cdot10^{-4}E)^{-0.4}(cm^2\cdot sec\cdot sr)^{-1} \quad [15]$$

$$I(>E/TeV)=3.30\cdot10^{-4}\cdot(E/0.1)^{-1.70}\cdot(1+6\cdot10^{-4}E)^{-0.4}(cm^2\cdot sec\cdot sr)^{-1} \quad [16]$$

Points of nucleus spectrum steepening are proportional to nucleus charges.

5. SPECTRA OF HADRONS AND ELECTROMAGNETIC COMPONENT

The first data to be described by any model are spectra of single particles. Intensities and slope indexes of electromagnetic (EM) particles (hereafter, called γ-quanta) and hadrons are very sensitive to $K_{inel}^{h\text{-}air}$ and $\sigma_{inel}^{h\text{-}air}$ as well as to spectra of secondaries, πICE process and so on. Up to now these problems have, in fact, been analyzed only by means of analytical calculations which cannot give quantitative predictions of characteristics of γ-h families and take some methodical problems into account. On the other hand, the Monte-Carlo method is not used, practically, to calculate single component intensities. As a result, there has not been any model so far which describes simultaneously both single components and family characteristics.

The intensity and slope indexes of γ-component at the Pamirs level have been calculated by means of MCO [7] for PCR spectrum by [15]. One can see from Table 5.1 including also results [39,40] that the experimental value β_γ [1] in the energy interval from 5 TeV up to $\simeq$ 100 TeV is close to the simulated one.

However, an essential part of spots rising with energy is

produced by electromagnetic cascades from air, but not single γ-quanta [37]. It is impossible to separate these types of events because of limited sizes of measuring diaphragms. It can lead to the energy overestimation and spectrum hardening [18]. A difference between the real and measured index values equals to $\Delta\beta_\gamma=\beta_\gamma^{real}-\beta_\gamma^{meas}\approx 0.15\div0.2$, i.e. the real value to be compared with analytical predictions is $\beta_\gamma^{real}\approx 2.25-2.3$ [18].

In part, this problem could be connected with the following problem. Quasi-scaling models predict a reasonable index values and too high family intensities in comparison with the experimental data, whereas models assuming strong scaling violation predict the intensity close to the experimental one but too big index values [44]. This contradiction can be reduced taking the above effect into account in favor of models with scaling violation.

The situation with the hadron spectra is not evident also. In Table 5.2 the experimental slope indexes β_h of various authors in the energy interval from E_{thr} up to ≃ 100 TeV are listed. Spectra obtained by means of Pb-chambers are steeper, in average, than ones obtained by C-chambers are. It could be explained by the following methodical reasons.

Table 5.3 displays the relative intensities and slope indexes of vertical integral spectra of different types of hadrons at the Pamirs level calculated with MCO taking into account the hadron registration efficiency [8] in C-EC. The indexes of spectra at E_h > 20 TeV above chambers are listed in third column. The efficiency rises from ≈0.1 at $E_h\geq3$ TeV to ≈0.7 at $E_h\geq70$ TeV [8]. As a result, the measured spectrum is harder and not really power law one. It is seen from last three columns, where the index values are shown for various minimal energies. Even at E_h^γ > 20 TeV the "measured" spectra are harder than the arriving hadron spectra. In Pb-chambers this effect has to be weaker and, as a result, a difference between the indexes of measured and real spectra has to be less, not more than ≈0.05. From Tables 5.2 and 5.3 one can see that the real hadron spectrum index can be $\beta_h\cong 2.1$, i.e. close to the simulated one.

In the case of lead chambers the experimental and simulated results agree also rather well both in intensities and absorption path values λ_{abs}^{h-air} (100±6 and 98±2 g/cm^2 at $E_h^\gamma \geq 6.3$ TeV

correspondingly). Note that the simulated value λ_{abs}^{h-air} [3] is obtained from intensity values at different altitudes whereas the experimental one is calculated from the angular distribution and can depend on accuracy of the energy measurement at large angles.

However, the most important result of the simulation concerns the equality of slope indexes of both the γ-component and total hadron spectrum. It contradicts the results of [18,19] obtaining by means of a new method the difference equaled to $\Delta\beta=\beta_\gamma-\beta_h \approx 0.3\div0.4$. Taking into account the energy dependence of hadron registration efficiency, we can assume $\Delta\beta \approx 0.2$. This difference is very important, since it is possible only in models with strong scaling violation in the fragmentation region [38,52]. In models with a moderate scaling breaking $\beta_\gamma \leq \beta_h$ [38,52].

Thus the QGSM-based model MC0 cannot explain differences between slope indexes of γ- and hadron components. How can the model be changed to make its predictions agree with the data [18,19] ? One can see from Table 5.3 that various hadron components have different slope indexes. The pion spectrum is steep, but rather not enough. One could think that the γ-spectrum has to be parallel to the pion one but it is essentially harder. It can be explained in the following way. First, the main part of γ-quanta is produced by nucleons. Their spectrum is harder than the pion one. Second, the observed EM-component originates from γ-quanta generated at some effective altitude above chambers where the pion spectrum is harder. The scaling-like EM-cascade development produces the γ-spectrum at the observation level with the same slope. To steepen the γ-spectrum it is necessary to steepen the neutral pion spectrum in hadron- nucleus collisions more strongly than in QGSM [5]. This model modification can be connected with a relative decrease of K_{inel}^{h-air} in the case of the invariable multiplicity dependence on energy.

Table 5.1.The slope indexes β_γ of vertical simulated and experimental integral γ-spectra at E > 5 TeV.

Type of data	β_γ(>5 TeV)	Ref.
Simulation	2.11±0.03	[7]
Experiment	2.07±0.06	[1]
	2.00±0.08	[39]
	2.00±0.05	[40]

Table 5.2. The slope indexes β of the experimental integral hadron spectra at $E_h^\gamma > E_{thr}$.

E_{thr}, TeV	$\beta_h(E_h^\gamma > E_{thr})$	Chamber type	Ref.
5.	1.96±0.06	Pb	[1]
6.3	2.01±0.08	Pb	[3]
5.	2.03±0.08	Pb/Fe	[39]
5.	2.0 ±0.1	Pb	[40]
20.	1.90±0.15	C	[19]
7.	1.90±0.1	C	[41]

Table 5.3.The simulated slope indexes $\beta(E_h, E_h^\gamma > E_{thr})$ and relative intensities $I_h(E_h > 20$ TeV) of integral hadron spectra.

Hadron type	I_h (%)	β			
		$E_h > 20$ TeV	$E_h^\gamma > 3$ TeV	$E_h^\gamma > 8$ TeV	$E_h^\gamma > 20$ TeV
all	100	2.08±0.01	1.69±0.02	1.85±0.01	1.95±0.01
nucleons	60	2.10±0.01	1.61±0.02	1.83±0.01	1.92±0.01
Λ/Σ	2	1.42±0.02	1.14±0.02	1.25±0.05	1.30±0.05
pions	25	2.22±0.01	1.76±0.02	1.95±0.02	2.25±0.03
kaons	13	2.03±0.01	1.54±0.01	1.78±0.02	1.84±0.03

6. CHARACTERISTICS OF GAMMA-RAY - HADRON FAMILIES WITH $\Sigma E_\gamma > 100$ TeV

6.1. Intensity of gamma-ray families

In Table 6.1 experimental and model intensities of γ-families detected with Pb-EC [3] are given. The good agreement is darkened by poor statistics only. The model MQ (MQ1) predicts the family flux with $\Sigma E_\gamma = 80 \div 400$ TeV ($R_\gamma \leq 15$ cm, $E_\gamma \geq 8$ TeV) $I_{fam}^{simul} = 0.9 \pm 0.07$ (0.6±0.1) $(m^2 \cdot year)^{-1}$ for C-EC [9] and PCR [15] whereas the experimental flux $I_{fam}^{exper} = 0.45 \pm 0.05$ $(m^2 \cdot year)^{-1}$ [54]. The difference of simulated intensities is due to difference in πICE probability W_c values. Decrease of W_c to ≈ 0.3 can make predictions agree with I_{fam}^{exper}. Note that a large degree of the azimuthal asymmetry of γ-h families (Sect. 8) is the only serious argument in favor of existence of πICE process at superhigh energies. An asymmetry explanation with processes different from πICE can do it to be superfluous to describe the soft interactions.

Table 6.1.Total and vertical experimental and calculated intensities of γ-families in Pb-chambers [3]. $E_{thr} = 6.3$ TeV.

Type of data	$I(\Sigma E_\gamma > 100$ TeV)		Ref.
	total $(m^2 \cdot year)^{-1}$	vertical $(m^2 \cdot year \cdot sr)^{-1}$	
experiment	0.38±0.10	0.67±0.15	[3]
MC0	0.37±0.02	0.70±0.08	

6.2. Angle distribution of gamma-ray families

As it has been mentioned above (Sect.5) experimental and simulated results accumulated by means of lead chambers on hadron angle distributions agree rather well in mean absorption path value [3] being about 100 g/cm^2. The absorption path λ_{abs}^{fam} of γ-families with $\Sigma E_\gamma > 100$ TeV by the Collaboration "Pamir" is 73±8 g/cm^2 at $\vartheta<30^\circ$ [62]. This value can rise up to the upper limit equal at $\vartheta<45^\circ$ to 80±5 if various methodical factors will be taken into account [62]. This value is rather larger than the corresponding value predicted by MQ, i.e. 70 g/cm^2, but essentially smaller than 100 g/cm^2 obtained in experiments at Mt.Chacaltaya and Canbala. Thus, QGSM-based models predicts too strong family absorption in the atmosphere.

6.3. Transversal characteristics of γ-h families

In Table 6.2 average transversal characteristics of γ-h families with ΣE_γ = 100-400 TeV are listed. One can see a rather good agreement between experimental and simulation results within the error limits for both Pb- and C-chambers. Results [42,48] show that at ER > 1.5 GeV·km experimental ER-distributions are situated higher than simulated ones. It can confirm a hypothesis about appearance of a new processes with large $\langle p_t \rangle$ value at $E_0 \gtrsim 10$ PeV. However, statistics is not large, so this result is preliminary.

Table 6.2.Average transversal characteristics of γ-h families; ΣE_γ=100-400 TeV; E_{thr}=6.3 TeV (* - E_{thr}=4 TeV; $^\#$ - E_{thr}=10 TeV)

Type of data	Type of EC	$\langle \overline{R_\gamma} \rangle$ mm	$\langle \overline{E_\gamma R_\gamma} \rangle$ TeV·mm	$\langle \overline{R_h} \rangle$ mm	$\langle \overline{E_h^\gamma R_h} \rangle$ TeV·mm	Ref.
experiment	Pb	20±4	273±47	26±5	375±70	
MC0 K_γ^1				27±2	350±30	[3]
MC0 K_γ^2		21±1	269±18	32±2	404±35	
experiment	C	20±1*		23±2$^\#$		
MQ		23±1*		20±3$^\#$		[9]

6.4. Longitudinal characteristics of families

The spectrum of family hadrons is more sensitive to interaction parameters than the γ-spectrum. Both in MQ [4] and MCO [24] it agrees well with the experimental data. It depends on family-hadron composition (mainly, on nucleon fraction) as well as $K_{inel}^{h\text{-}air}$ and $K_{inel}^{h\text{-}chamber}$. Generators MQ, MSF, and MCP predict very different spectra "above" chambers (the difference can be as large as one order). The "measured" spectra in this models are much closer if one uses the same K_{inel} values in chamber simulations which are used in air cascade simulations. The spectra can differ very much in the contrary case as it is seen well from comparison of [9] and [46]. Taking into account that a large fraction of family hadrons consists of kaons (23%) and nucleons (23%) while the pion's one is 54% [3], it would be possible to vary the pion spectrum slope within certain limits without contradictions with the experimental data.

6.5. Multiplicity and correlations

In Table 6.3 the multiplicity $\langle n'_\gamma \rangle$ of "rejuvenated" events (i.e. families consisting of cascades ordered with respect to energy decrease and including particles with energy $E_i \geq 0.04 \sum_{j=1}^{i}{}' E_j$ only) and hadron multiplicity $\langle n_h \rangle$ of families with energy ΣE_γ = 100 - 400 TeV for different installations and simulations are listed. The average ratio of γ-family energy to total event energy detected in chambers ($Q_\gamma = \Sigma E_\gamma / (\Sigma E_\gamma + \Sigma E_h^\gamma)$), the fraction W_Q of families with Q>0.9 and the fraction W_n of families with the hadron number n_h=0 are given as well.

One can see a rather good agreement of the experimental and simulation results both for Pb- and C-EC, excluding absence of events with $n_h \geq 10$ among MQ-simulated events. This problem is not connected with QGSM properties as MCO simulates families of such multiplicity. However, the both models, as well as other models, cannot explain Centauro-like events with extremely large n_h.

Summing up, both the models MQ and MCO describe rather well longitudinal and transversal characteristics of γ-h families with ΣE_γ=100-400 TeV. However, the single-component spectrum slopes predicted by QGSM-based models differ from the experimental data.

Table 6.3.Values of $\langle n'_\gamma \rangle$, $\langle n_h \rangle$, $\langle Q_\gamma \rangle = \langle \Sigma E_\gamma / (\Sigma E_\gamma + \Sigma E_h^\gamma) \rangle$, $W_Q(Q>0.9)$ and $W_n(n_h=0)$ for γ-h-families with energy ΣE_γ=100-400 TeV and E_{thr}=6.3 TeV (* - E_{thr}=4 TeV; $^\#$ - E_{thr}=10 TeV).

Type of data	EC	$\langle n'_\gamma \rangle$	$\langle n_h \rangle$	$\langle Q_\gamma \rangle$	$W_Q(Q>0.9)$	$W_n(N_h=0)$	Ref.
experim.	Pb	10.6±.6*	2.2±.3	0.83±.06	0.44±.09	0.20±.07	
MCO K_γ^1			2.0±.2	0.86±.01			[3]
MCO K_γ^2		10.7±.3*	2.6±.2	0.82±.01	0.40±.04	0.18±.03	
experim.	C	10.0±.2*	0.92±.1$^\#$		0.63±.04*	0.54±.03$^\#$	
MQ		9.8±.2*	0.9 ±.1$^\#$		0.65±.03*	0.48±.04$^\#$	[9]

7. SUPERFAMILY CHARACTERISTICS

The main part of information on interactions at energies higher than 10^{16} eV is is accumulated by means of analysis of γ-superfamilies with ΣE_γ>500 TeV obtained in a lot of works [1,25,53,55-61]. Summing up their results, the QGSM-based model describe rather well longitudinal and transversal characteristics of the periphery of superfamily γ-component corresponding to $\lg(E_0/1\ \text{TeV}) \approx 4.2 - 5.1$ [23]. Both the central part of high energy concentration including the halo phenomenon and the hadron component of these events are not investigated yet in detail. We will use below some results of these works.

8.AZIMUTHAL EFFECTS IN FAMILIES

8.1.Brief introduction

Observation of some essential excess of the γ-family azimuthal effects over the simulated background (azimuthal asymmetry, binocular events, alignment etc.) stimulated attempts to explain the phenomenon either by trivial kinematics effects [67,68], or by means of gluon jet generation [64], or considering it as a result of rupture of quark-gluon string semihardly stretched between fast constituents of the projectile hadron [65] or in the framework of a quark compositeness model [63]. However, a final conclusion is not obtained yet.

Specific parameters, namely $\alpha_N = \sum_{i \neq j}^{N} \text{Cos}\ 2\varepsilon_{ij} / \{N \cdot (N-1)\}$ [28,29] and $\lambda_N = \sum_{i \neq j \neq k}^{N} \text{Cos} 2\varphi^k_{ij} / \{N \cdot (N-1) \cdot (N-2)\}$ [32] are used by the Collaboration "Pamir" to calculate the azimuthal asymmetry and

alignment of family particles respectively. Their values equal to $\alpha_N = \lambda_N = 1$ for N points placing in a straight line and decrease to $\alpha_N \approx \lambda_N \approx -1/(N-1)$ in the isotropic case. To calculate α_N angles ε_{ij} between vectors drawn from the energy-weighed event center to i-th and j-th points are used whereas to compute λ_N angles φ^k_{ij} between vectors from k-th point to i-th and j-th points are calculated.

Table 8.1. Experimental and simulated values of $\langle\alpha\rangle$ for families with ΣE_γ=100-400 TeV in Pb-EC ($n_\gamma \geq 5$) and C-EC ($n_\gamma \geq 3$).

Type of data	Type of EC	E_{thr}, TeV		Ref.
		4	6.3	
experiment	Pb	0.19±0.04	0.24±0.05	
MCO		0.15±0.02	0.19±0.02	[3]
experiment	C	0.29±0.02		
MQ		0.33±0.02		[9]

8.2.Azimuthal asymmetry

Attempts to analyze the azimuthal asymmetry in terms of α_N in the framework of the semi-hard jet generation and πICE process were made in [30]. However, the experimental asymmetry degree can be explained only by means of πICE process [9]. The main reason is a slower development of subcascades from γ-quanta carrying the considerable part of energy of parent pions. Thus, the subcascades can begin higher and go farther from the NEC axis magnifying the event asymmetry. It is illustrated by Table 8.1 listing the experimental and model values of $\langle\alpha\rangle$. One can see some difference between Pb- and C-EC experimental values. It could be explained by means of different selection criteria of the family particle numbers, various types of fluctuations of hadron energy fractions transferred into γ's and measured by means of different methods. It seems that the value predicted by MCO is smaller than the experimental one. No doubt, MCO considering the jet generation but not πICE predicts the smaller asymmetry degree than MQ including πICE does. This difference can be particularly reduced if energy measurement errors would be taken into account in Pb-EC. However, the rate of πICE process used by MQ is not observed in accelerator experiments at relatively high energies [31]. A resolution of this contradiction could be found in some new way connected probably with an explanation of the alignment phenomenon which cannot be explained by means of πICE.

8.3.Alignment

The phenomenon of family object alignment in a straight line is another azimuthal effect manifestation discovered first for multicore halo events [32] and then for the so-called energy distinguished cores (EDCs) [33]. An experimental probability $W(\lambda_4>0.8)$ of finding aligned four-EDC events with $\Sigma E_\gamma>700$ TeV in Pb-EC and C-EC is 0.43±0.17 [62] and 0.26±0.09 [43] respectively while the background value is 0.08±0.02 only [33].

In [34] three possible causes of this phenomenon were analyzed, namely, fluctuations, external fields, and, finally, hadron interaction physics.

Two experimental family set under consideration with $\Sigma E_\gamma \geq 700$ TeV consist of 14 [62] and 35 [43] events including 6 (A) and 9 (B) aligned events respectively. To test the first effect origin, 500 (A) and 250 (B) family sets involving the corresponding event numbers were simulated for either case. Resulting distributions of the number of aligned γ-h families $N_{fam}(\lambda_4>0.8)$ in each of the sets are shown in Fig.8.1 (A,B). In either case one cannot see a single simulated set coinciding with the experimental ones. Thus, the fluctuation origin of the phenomenon is improbable.

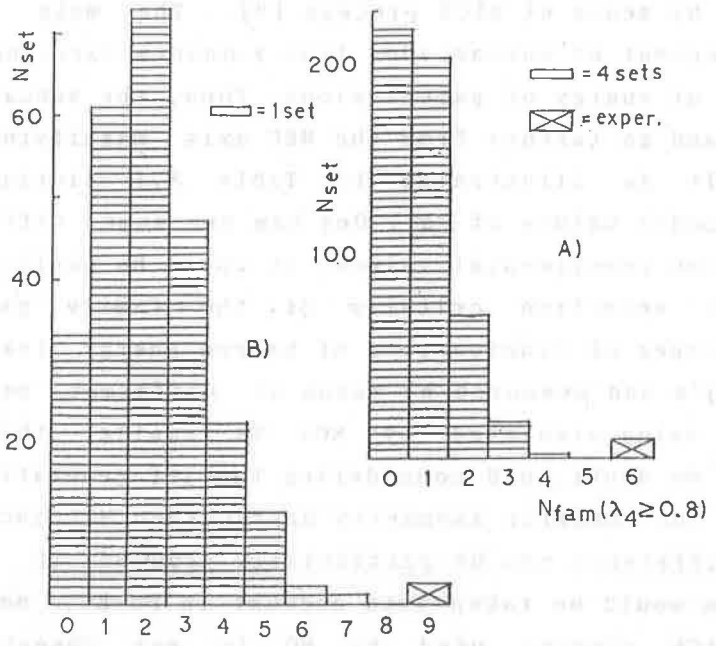

Fig.8.1.Distributions of family sets as functions of the number of aligned γ-h families $N_{fam}(\lambda_4>0.8)$ in each of the sets. Each of the rectangles corresponds respectively to four (A) or one (B) family set consisting of 14 (A) or 35 (B) events simulated by MCO. Rectangles marked as 'E' correspond to the experimental sets.

To analyze the phenomenon external origin, two factors capable of producing azimuthal effects, namely, the Earth's magnetic field and atmospheric electric fields were considered. As it is seen from Table 8.2 the magnetic field cannot explain the effect, independently from primary particles. Here the notations are the following:

EMD denotes the projectile nucleus electromagnetic dissociation in electric fields of air nuclei.

MF denotes the Earth's magnetic field.

Two models were analyzed, namely the vertical and horizontal electric fields with gradients of 1 and 2 GV respectively, i.e. close to maximal values possible in the atmosphere. In Table 8.3 results for cascades initiated by protons are given, for gammas and hadrons separately. One can see that the fields are not too strong to eliminate chaotic transversal hadron motion whereas the vertical field can magnify the alignment of γ-quanta essentially.

To analyze the hadron interaction origin, simulations were made by means of various NEC development models. In Table 8.4 simulation results [34] for primary nucleons are listed. Abbreviations of model variants taken into account are as follows.

ALG denotes a particle coplanar generation of the usual $<p_t>$.

DDD denotes the double diffraction dissociation of projectiles with a large momentum transferred into clusters decaying into secondaries with the usual $<p_t>$ in the cylindrical phase space.

ISD denotes the single diffraction dissociation of the enlarged cross section (the usual one times 10).

PNP denotes the photonuclear processes of the weakly rising cross section [14] taking place in EM cascades.

ROT denotes the high-spin rotation of the noninteracting part of the projectile nucleus with its following coplanar destruction.

SHDID denotes the semihard diffractive inelastic dissociation with the momentum squared $Q_t^2 \approx (n \cdot \mathrm{GeV/c})^2$ transferred to the projectile hadron and rupture of a quark-gluon string stretched between semihardly scattered fast constituents [65].

X denotes unknown long - flying component having a rather small cross section $\sigma_{inel}^{X\text{-}air} \approx 0.2 \cdot \sigma_{inel}^{p\text{-}air}$ and interacting through the coplanar hadron generation of secondaries with $<p_t^X> \approx 10 \cdot <p_t>$.

One can see from Table 8.4 that only a process of secondary particle alignment with the usual $<p_t>$ together with very large

diffraction cross-section can increase the fraction of aligned events a little. The same conclusion can be derived for cascades initiated by primary nuclei and gamma-quanta.

It is possible to explain the effect assuming [34] existence of a hypothetical particle with $\lambda_{int} \approx n \cdot \lambda_{int}^{p-air}$ (for theoretical suggestion see, e.g., [66]) interacting through the coplanar particle generation. However, the experimental zenith angular distributions of both aligned and usual families [43] does not confirm this hypothesis.

The experimental results can be described [69], in part, in the framework of SHDID model [65]. However, it is necessary to assume additionally that the normal-to-string momentum of secondaries is ≈0.02÷0.05 GeV/c, i.e. several times lesser than the corresponding value in e^+e^- collisions at the same invariant energies, whereas the cross section of SHDID interactions $\sigma_{shdid}(Q_t \geq 8 \text{ GeV/c}) \approx 0.05 \cdot \sigma_{inel}$ and the average transversal momentum transferred to a constituent quarks $\langle Q_t \rangle \approx 5 \div 6$ GeV/c.

In this connection a hypothesis [47] is of interest assuming that the alignment is a result of new strong interactions above the electroweak scale at energies $\sqrt{s} \gtrsim 4$ TeV characterized by very large transverse momentum as well as generation of heavy hadrons interacting with small K_{inel}

Summing up, the alignment also is an evidence in favor of processes with large $\langle p_t \rangle$ taking place at super high energies.

Table 8.2. Values of $\langle \lambda_4 \rangle$ and $W(\lambda_4 > 0.8)$ for all particles of γ-h families initiated by primary protons, α-particles and γ-quanta. Statistical errors are lesser than 0.01.

Primary particle	p		α			γ	
Model	MCO	+MF	MCO	+MF	+MF+EMD	Pure EPhC	+MF
$\langle \lambda_4 \rangle$	0.23	0.22	0.21	0.21	0.22	0.24	0.28
$W(\lambda_4 > 0.8)$	0.06	0.05	0.05	0.04	0.05	0.07	0.08

Table 8.3.The same as in Tab. 8.1 separately for hadrons and γ-quanta of γ-h families initiated by protons. Horizontal and vertical electric fields are taken into account.

Field	Horizontal		Vertical	
Particles	hadrons	γ-quanta	hadrons	γ-quanta
$\langle \lambda_4 \rangle$	0.24 ±.01	0.31 ±.02	0.28 ±.01	0.39 ±.02
$W(\lambda_4 > 0.8)$	0.06 ±.01	0.09 ±.02	0.09 ±.01	0.16 ±.02

Table 8.4. Values of $\langle\lambda_4\rangle$ and $W(\lambda_4>0.8)$ for all particles of γ-*h* families initiated by primary protons, α-particles and X-component in the framework of various hadron interaction models at 350 g/cm^2 in the atmosphere for E_{thr}=200 TeV [34].

Primary particle	p				α	γ		X
Model	+DDD	+ALG	+ISD	+ISD+ALG	+ROT	+PNP	+PNP+ALG	
$\langle\lambda_4\rangle$	0.21	0.27	0.21	0.28	0.22	0.24	0.26	0.69
$W(\lambda_4>0.8)$	0.05	0.09	0.06	0.10	0.06	0.08	0.08	0.56

9. DISCUSSION

There are some indications of possible differences between certain of interaction characteristics at $E \gtrsim 10^{15}$ eV and the QGSM predictions. It seems that the leading hadron spectra are probably harder. The registration of the *Elena* event [26] with the distinct hadron leader may be a circumstantial evidence for this point of view. The relative intensity of energetic hadrons with and without accompaniment has to be sensitive to this parameter [27].

Thus, one can propose some relative decrease of $K_{inel}^{h\text{-}air}$ and pion spectrum steepening in hadron interactions in comparison with QGSM predictions. How can these assumptions change results ?

As regards intensities of components, the proposed modifications act in the opposite directions. Thus it is possible to keep the calculated intensities close to the same values. Then the hadron spectrum has to be harder. So the PCR spectrum fit [16] would be more suitable. The single γ-spectrum has to be steeper.

The pion spectrum slope in families depends on model parameters rather weakly [9]. The arriving pion intensity will be larger if we decrease $K_{inel}^{\pi\text{-}air}$. However, it could be compensated by decreasing the energy transferred into γ's by interacting hadrons and steepening the pion generation spectrum. Therefore, the registered pion intensity would be almost the same if modifications are not very large. The only problem is a slope of the spectrum of the maximal hadron energy depending on $K_{inel}^{p\text{-}air}$ [9]. Its decrease has to lead to some spectrum hardening. However, for the accurate comparison with experimental data it is necessary to use, contrary to [9], the same model both for the atmospheric and chamber simulations. In this case a more slow increase of K_{inel} in comparison with the QGSM predictions will keeps the simulated spectrum within reasonable limits.

As regards lateral characteristics, the smaller K_{inel} the larger R_h. It does not contradict to experimental results.

The parameter $<n'_\gamma>$ is not very sensitive to moderate changes

It seems that $<n_h>$ and its fluctuations will be larger and the fraction of energy carried by hadrons will increase a little.

At last, azimuthal effects as well as some excess of wide families are an evidence in favor of a new channel appearing at $E \gtrsim 10^{16}$ eV, additional to traditional ones.

10.CONCLUSIONS

The total set of the Collaboration "Pamir" data corresponding to interaction energies $E \geq 10^{15}$ eV can be explained rather well by means of simulation algorithms based on the quark-gluon string model [5]. Nevertheless, it could be better described by means of an interaction model assuming the following changes in comparison with the above models.

- · a smaller $K_{inel}^{h\text{-}air} \lesssim 0.6$;
- ·· a steeper spectrum of the secondary particle generation;
- ··· appearance of a new channel characterized by a (very) large transferred momentum related to SHDID [65] or a new higher- color quark sector [47] at $E \geq 10^{16}$ eV
- ···· absence or small cross-section of πICE process
- ····· a PCR spectrum like to the fit [16] or more steep.

11.ACKNOWLEDGMENT

This work was supported, in part, by a Soros Foundation Grant.

References

[1] Pamir, Mt.Fuji and Chacaltaya Collaborations, Nucl. Phys. B191 (1981), 1; Bayburina S.G. *et al.*, Trudy FIAN (Proc.Lebedev Inst.) Moscow, v.154 (1984), 3 (in Russian)
[2] Dunaevsky A.M. *et al.*, Trudy FIAN (Proc.Lebedev Inst.), Moscow, v.154 (1984), 142 (in Russian)
[3] Pamir Collaboration. Proc. XXII ICRC, Dublin (1991), v.4, 113
[4] Pamir Collaboration. Proc. XXII ICRC, Dublin (1991), v.4, 121
[5] Shabelsky Yu.M. Z.Phys.C, v.38, No 4 (1988), 569
[6] Dunaevsky A.M., Pluta M. and Slavatinsky S.A. Proc. 5th ISVHECRI, Lodz, Poland (1988), p. 143-160
[7] Mukhamedshin R.A. Proc. XXI ICRC, Adelaide (1990), v.9, 28 Mukhamedshin R.A. and Krys A., Prepr. Lodz Univ. No 13.42/90
[8] Dunaevsky A.M. and Zimin M.V. Proc. 5th ISVHECRI, Lodz,Poland (1988), 93-111
[9] Dunaevsky A.M. *et al.* Proc.XXII ICRC, Dublin (1991), HE 1.3.5
[10] Azimov S.A. *et al.* Proc. XX ICRC, Moscow (1987), v.5, 304
[11] Denisova V.G. *et al.* Proc. XX ICRC, Moscow (1987), v.1, 390

[12] JACEE Collaboration.Proc. XXII ICRC, Dublin (1991), OG 6.1.21
[13] Freudenreich H.T., Mincer A.I., Berley D. *et al.* Phys.Rev.D, v.41, No 9, 2732-2750
[14] Dyakonov M.N. *et al.*Proc. XXII ICRC, Dublin (1991),OG 6.1.4; Bordoloi T.C. *et al.* Proc. XXII ICRC, Dublin (1991), OG 6.1.8
[15] Nikolsky S.I. Proc. 6th ISVHECRI, Tarbes, France (1990)
[16] Erlykin A.D. Thesis Phys. D-r degree, Moscow, FIAN (1989)
[17] Erlykin A.D. *et al.* J.Nucl.Phys., v.45, 4, 1075
[18] Bialobrzeska H. *et al.* Proc. 22nd Int.Pamir Workshop VHECRI, Lodz, Poland (1991), v.1, 28
[19] Malinowski J.,D.Sangwal, A.Tomaszewski. Proc.22nd Int. Pamir Workshop VHECRI, Lodz, Poland (1991), v.1, 57-60
[20] Chubenko A.P., Nikolsky S.I. Proc.XXI ICRC, Adelaide (1990), v.8, 202-205
[21] Arabkin V.V. *et al.*Proc. XXII ICRC, Dublin (1991), v.4, 141
[22] Mukhamedshin R.A. Ph.D. Thesis, Moscow,1982
[23] Pamir Collaboration. Proc. XXII ICRC, Dublin (1991), v.4, 129
[24] Pamir Collaboration. Proc. 22th Int. Pamir Workshop, Bull.Soc.Sci.Lettr.Lodz, Poland (1992), v.XII, N 111
[25] Amineva T.P. *et al.*Proc.5th ISVHECRI, Lodz, Poland (1988), 24
[26] Borisov A.S. *et al.* Preprint FIAN No 208, Moscow (1989)
[27] Pamir Collaboration. Proc. XX ICRC, Moscow (1987), 285
[28] Azimov S.A. et al. ZNUŁ, ser.II, zezs. 60 (1977), 281-282
[29] Pamir Collaboration. Proc. XVII ICRC, Paris (1981), v.11, 156
[30] Azimov S.A. *et al.* Proc.XVIII ICRC, Bangalore (1983), v.5,458
[31] Ljung D. *et al.* Phys.Rev.D, v.15, No 11,3163
Aguilar - Benitez M. *et al.* Z.Phys. C34 (1987), 419;
[32] Pamir Collaboration.Proc.4th ISVHECRI, Beijing (1986), 4-29
[33] Amineva T.P. *et al.* Prepr. INP No 91 - 5/209 (1991)
[34] Mukhamedshin R.A. Proc. 23rd ICRC, Calgary (1993) v.4, p.100
[35] Fedorova G.F. and Mukhamedshin R.A. Proc. 22nd Int. Pamir Workshop,Bull.Soc.Sci.Lettr.Lodz, Poland (1992) v.XIII, N 130
[36] Hasegava S. Centauro species in cosmic ray observation, ICR-Report-151-85-5, Tokyo, Japan,1987
[37] Borisov A.S. *et al.* Preprint FIAN No 212, Moscow (1987)
[38] Kasahara K. ICR - Report - 62 - 78 - 6, Tokyo, Japan, 1981
[39] China-Japan Emulsion Chamber Collaboration. Proc. XIX ICRC, La Jolla (1985), v.6, 204.
[40] Mt.Fuji Collaboration.Proc.XIX ICRC, La Jolla (1985), v.6,208
[41] Cananov S.D. *et al.* Proc. XIX ICRC, La Jolla (1985), v.6, 216
[42] Zhdanov G.B. *et al.*Preprint FIAN No 112 & 114, Moscow (1991)
[43] Pamir Collaboration.Proc.8th ISVHECRI, Tokyo (1994)
[44] Chacaltaya and Pamir Collaborations. Proc. XXII ICRC, Dublin (1991), v.4, 93
[45] Capdevielle J.N. J.Phys.G 15 (1989) 909
[46] Denisova *et al.* Proc. 7th ISVHECRI, Ann-Arbor (1991)
[47] White A.R.Proc.8th ISVHECRI, Tokyo (1994); Int.J.Mod.Phys.A8, 4755 (1993)
[48] Denisova V.G.and Zhdanov G.B. Proc.XXI ICRC, Adelaide (1990), v.9, 215
[49] Bakatanov V.N. *et al.* Pis'ma ZhETPh (Sov. Phys.-Lett.J. Exp. Theor.Phys.), v.56, 5 (1992), 237
[50] Kalmykov N.N. *et al.*Proc. 23rd ICRC, Calgary (1993) v.4, 239
[51] Ivanenko I.P. *et al.* Pis'ma v ZhETPh (Sov. Phys.-Lett.J. Exp. Theor.Phys.), v.56, 4 (1992), 192
[52] Ivanenko I.P. *et al.* Yadernaya Fisika (Soviet Nucl.Phys.), v.29 (1979) p.694-707
[53] Pamir Collaboration. Proc.XXI ICRC, Adelaide (1990), v.8, 227
[54] Pamir Collaboration. Proc.Interregional Conference on Cosmic

Rays, Samarkand, Uzbekistan (1992)
[55] Pamir and Chacaltaya Collaborations. Proc.XXI ICRC, Adelaide (1990), v.8, 243
[56] Dunaevsky A.M., Pluta M.Proc.XXI ICRC,Adelaide (1990),v.8,274
[57] Pamir Collaboration. Proc.5th ISVHECRI, Lodz,Poland (1988),30
[58] Genina L.E. *et al.* Proc. XVII ICRC, Paris (1981), v.11, 145
[59] Ivanenko I.P. *et al.* Proc. XV ICRC, Plovdiv (1977), v.7, 276
[60] Gulov Yu. A. *et al.* Preprint FIAN No 143 Moscow (1983)
[61] Pietrzak T.,Wrotniak J. Proc.XVI ICRC, Kyoto (1979), v.7, 193
[62] Ivanenko I.P. *et al.*:1992, Pis'ma ZhETPh (Sov. Phys.-Lett.J. Exp.Theor.Phys.) v.50, 11, 2125
[63] Cao Z. *et al.* Phys.Rev.Lett.72, 1794 (1994)
[64] Halzen F. and Morris D.A., Phys.Rev.D, v.42, N 5,(1990) 1435
[65] Royzen I.I.Prepr. LPTHE 92/57,Univ.de Paris XI,France (1992); to be published in Mod.Phys.Lett.A,1994
[66] Bazhutov Yu.N. *et al.*Preprint CNIIMASh, N 1, Moscow (1990)
[67] Zhu Q.-Q. *et al.*Proc.21st ICRC, Adelaide (1990) v.8, 306
[68] Smirnova M.D. and Smorodin Yu.A.Proc.21st ICRC, Adelaide (1990) v.8, 310
[69] Mukhamedshin R.A. Proc.8th ISVHECRI, Tokyo (1994)